

# Design optimization of nozzle configuration in deep sea double-jet hydraulic collector

Jiancheng Liu<sup>1</sup>, Boying Liu<sup>2</sup>, Lei Li<sup>1,\*</sup>, Jiakang Wei<sup>1</sup>, Fangjie Zhai<sup>2</sup>, Xiuzhan Zhang<sup>1</sup>, Hao Li<sup>1</sup>, Yong Ma<sup>2,3,\*</sup>

<sup>1</sup>China Merchants Marine and Offshore Research Institute Co., Ltd., 518067 Shenzhen, China

<sup>2</sup>School of Ocean Engineering and Technology, Sun Yat-sen University, 519082 Zhuhai, China

<sup>3</sup>Southern Marine Science and Engineering Guangdong Laboratory, 519080 Zhuhai, China

**Abstract:** The ocean floor harbors abundant mineral resources, making seabed ore collection technology a prominent research area for scholars worldwide in recent years. In order to further explore the ore collection characteristics of the double-jet hydraulic collector, a numerical simulation method is employed to construct a numerical model, optimize the structure of front and back jet nozzle of the collector, and analyze the effects of circular tube nozzle and blade nozzle, different diameter of circular tube nozzle and nozzle axis distance on the collection efficiency and disturbance of the collector. It is concluded that the double-jet hydraulic collector achieves optimal collection performance when the circular tube nozzle has a diameter of 14 mm and the nozzle axis distance is twice the diameter of the round tube, and higher flow rates are better for collecting nodules but also increase environmental disturbance.

## 1. Introduction

There are abundant mineral resources such as polymetallic nodules, polymetallic sulfides and cobalt-rich crusts at the bottom of ocean. The exploitation and utilization of marine mineral resources is one of the effective means to solve the crisis of depletion of land mineral resources. As the most widely distributed and the largest reserves of seabed mineral resources, polymetallic nodules are widely used in electronic equipment and other fields, and have great mining and utilization value[1].

Polymetallic nodules are usually semi-buried on the seafloor surface and need to be collected through suitable collection methods. The existing acquisition technologies include mechanical, combined mechanical-hydrodynamic and hydrodynamic. According to the existing research results [2,3], mechanical and combined mechanical-hydraulic technologies have problems such as large damage to the seabed environment and easy wear of parts. Compared with the first two technologies, hydraulic acquisition technology has a simple device structure, high reliability, and meets the needs of long-term continuous work, which can be further subdivided into suck-up-based collection type, Coanda-effect-based collection type, and double-jet hydraulic collection type. Among them, the double-jet hydraulic collector has less energy consumption [4], and has greater commercialization potential. It has been a research hotspot of experts and scholars from various countries in recent years.

For the double-jet hydraulic collector, the collection efficiency and environmental disturbance are studied mainly through the combination of numerical simulation

and experiment at present. Guan[5] and Yang[6] et al. found that the jets from the front and back nozzles of the device played an important role in collecting nodules. Zhang[7] and Liu[8] et al studied the nozzle inclination and jet flow rate of the nozzle, and proposed the geometric parameters of the device under high acquisition efficiency. At present, the research of dual-flow acquisition device mainly focuses on the shape of arc plate, nozzle inclination angle and the distance between front and back nozzles, etc. The research of nozzle geometry is relatively few.

In this paper, by using numerical simulation method, the nozzle configuration, circular tube nozzle diameter and nozzle axis distance are studied. We explore the optimal nozzle configuration and geometric parameters of the double-jet hydraulic collector, which can provide reference for the design and optimization of the deep-sea mining in the future.

## 2. Numerical simulation of deep sea mining

### 2.1. Numerical methods

In this study, the numerical simulation was carried out using STARCCM+ software, which mainly involved the interaction of fluid and particles. The fluid phase is controlled by CFD method and K-Epsilon turbulence model. The particle phase is regarded as discrete phase by using DEM method. When particles move in a fluid, Newton's second law and the equation of conservation of angular momentum should be satisfied. At the same time, the Hertz-Mindlin model is used to control the collision

\* Corresponding author: [lilei@cmhk.com](mailto:lilei@cmhk.com); [mayong3@mail2.sysu.edu.cn](mailto:mayong3@mail2.sysu.edu.cn)

between particles. Considering the effect of tangential force  $F_t$  and normal phase force  $F_n$  upon particle collision, a spring-damping model is simplified, as shown in Figure 1.

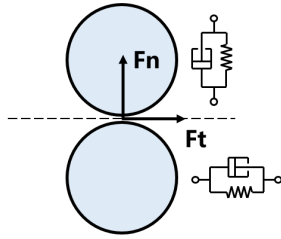


Fig.1. Particle impact spring-damping model

In addition, the particle-fluid two-phase coupling model (CFD-DEM) needs to be considered. The key problem is the momentum transfer between the continuous fluid phase and the discrete particle phase. This study mainly considers the drag model and the pressure gradient model:

$$F_{pl} = F_d + F_p \quad (1)$$

Where  $F_d$  represents resistance and  $F_p$  represents pressure gradient force. The resistance  $F_d$  and pressure gradient force  $F_p$  can be further calculated by the following formula:

$$F_d = \frac{1}{2} \rho_f C_d A_d \pi r^2 |u - v| (u - v) \quad (2)$$

$$F_p = -V_p \nabla p_{static} \quad (3)$$

Where  $\rho_f$  is the fluid density,  $C_d$  is the drag coefficient,  $V_p$  is the particle volume, and  $\nabla p_{static}$  is the gradient of static pressure in the fluid.

After that, the momentum transfer of the discrete particles relative to the continuous phase of the fluid is considered, mainly considering the drag force  $F_D$ , virtual mass force  $F_{VM}$  and lift force  $F_L$ :

$$F_{pl} = F_D + F_{VM} + F_L \quad (4)$$

## 2.2. Model design of double-jet hydraulic collector

The collection model selected in this study was simplified and designed according to the jet flushing hydraulic ore collection mechanism in the Exploitation of Deep Sea Solid Mineral Resources [9]. The cross-section view of the model is shown in Fig 2. The simplified components include the front and back nozzles, front curved baffle, transportation pipes and other structures. The front and back of the acquisition head are provided with nozzles. The Angle between the front nozzles and the ground is  $40^\circ$ , and the Angle between the rear nozzles and the ground is  $55^\circ$ .

The specific parameters involved in the process of numerical calculation are summarized as shown in Table 1:

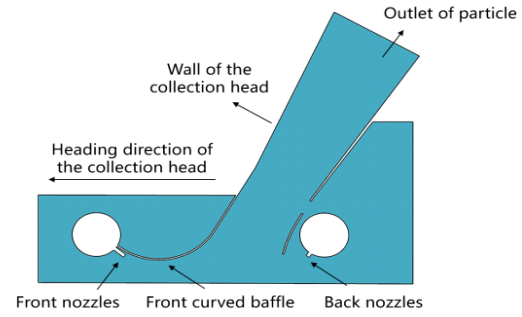


Fig.2. Cross-section view of the acquisition head model

Table 1. elect parameters for numerical simulation

Parameters	Implication	Value
$\rho$	Density of ore particles	2100 kg/m <sup>3</sup>
D	Diameter of the ore particle	0.05 m
A	Abundance of ore laying	15.264 kg/m <sup>2</sup>
g	Gravitational acceleration	9.81 m/s <sup>2</sup>
h	Height of the device from the bottom	0.09 m
d	Width of the collecting head	0.9 m

## 2.3. Computational domain and boundary conditions

In this study, StarCCM+ software was used for calculation and analysis. In order to improve the calculation efficiency, the calculation area is treated symmetrically, and the calculation time step is set to 0.005s. The fixed collecting head is not moved, and the x direction motion speed of water, simulated particles and seabed is set to 0.3m /s, and the movement process of the collecting head on the seabed is simulated by relative motion. In the calculation process, the particle diameter was set to 0.05m, and the particles entered the calculation domain from 1 second, and one group was released every 0.2 second, totaling 5 groups with 6 particles in each group, totaling 30 particles. The calculation domain and boundary conditions of the numerical simulation process are shown in Figure 3. Velocity inlet, pressure outlet, symmetric, non-slip wall and moving non-slip wall are set respectively.

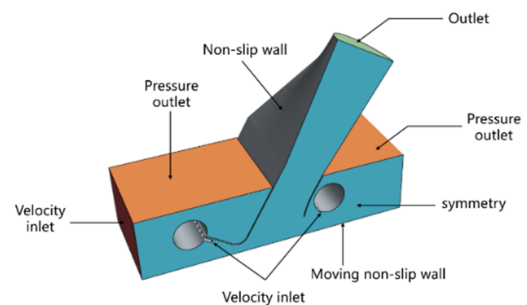


Fig.3. Calculation domain and boundary conditions

## 2.4. Mesh convergence analysis

To ensure the accuracy of numerical simulation and the grid scale does not affect the calculation results, this paper analyzes the convergence of 7 groups of grids of different

sizes, and chooses 0.005s as the calculated time step to calculate and detect the output mass flow rate of the device. The output results are shown in Figure 4. The simulation results show that the output mass flow rate basically converges when the number of grids exceeds 3 million. In order to improve the calculation efficiency and ensure the calculation accuracy, the number of grids selected in this paper is 3.35 million.

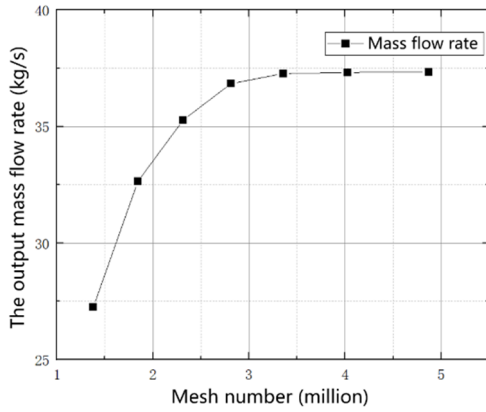


Fig.4. Grid convergence analysis

### 2.5. Numerical model validation

In order to verify the accuracy of the numerical calculation model. Using CFD-DEM model, the free falling model of small ball in water is established and calculated to monitor the resistance during free falling. As shown in Fig. 5, the calculated results were compared and analyzed with the control data [10]. It can be concluded that the numerical calculation resistance of this method is slightly less than the reference data, the overall calculation error is small, and the calculation model setting method is more reliable.

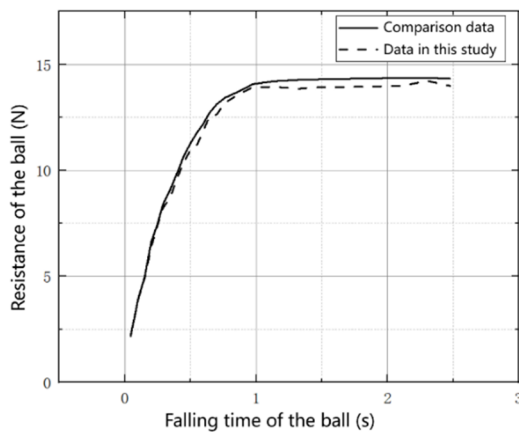


Fig.5. Comparison of numerical calculation results

### 2.6. Contents of numerical simulation research

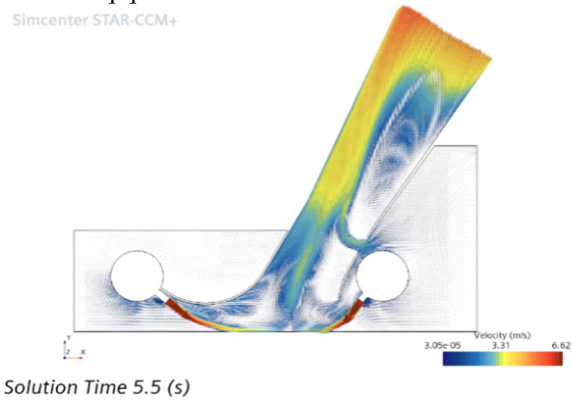
This study was carried out in clean water environment. By changing the shape of the nozzle in front and back of the collecting head, the influence of the plate nozzle and the round pipe nozzle on the collection performance of the device was explored. Further, the influence of the axial distance of the cylindrical nozzle on the acquisition

performance of the device is investigated under the same flow rate.

The collection performance was characterized by the number of particles collected and the collection time, and the scouring ability of the nozzle jet was characterized by recording the shear stress distribution of the jet impacting the seabed. Control the total input flow unchanged, calculate the nozzle design conditions of different sizes, explore the performance of corresponding collector.

## 3. Results and discussion

The fluid velocity vector diagram inside the collector head was obtained through numerical simulation, as shown in Figure 6. The two front and rear rows of jets converge in the center of the seabed bottom, forming an upwelling stream that effectively lifts ore particles to the ore collection pipe.



Solution Time 5.5 (s)

Fig.6. Internal flow field diagram of the acquisition head pipeline

Figure 7 shows the distribution of shear stress at the bottom of the seabed. Through analysis, it can be concluded that due to the larger inclination Angle of the rear nozzle, the disturbance to the seabed is more direct, and the shear stress generated by the rear nozzle is higher than that of the front nozzle. At the same time, due to the boundary effect of jet flow, the shear stress at the edge of the nozzle on the transverse fracture surface is larger.

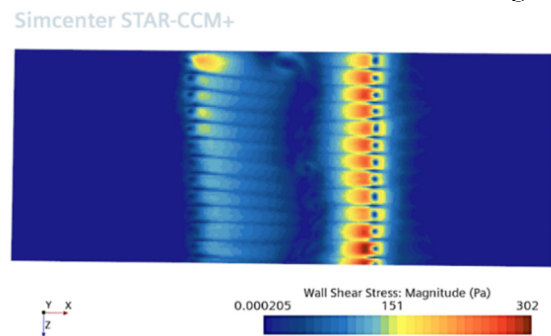


Fig.7. Distribution of shear stress at seabed bottom

Figure 8 shows the motion of particles in 1-2.4s. During the entire movement of being collected, the particles initially enter the flow field at a uniform speed from the left side. At 1.2s, the particles accelerate to move to the center of the collection head under the water jet. At 1.4s, the particles enter the upwelling area formed by the intersection of two sets of jets and begin to accelerate

upward. At 1.6s, some particles arrive at the exit and are successfully collected, 1.8-2.4s, and subsequent particles repeat the previous process and are gradually collected.

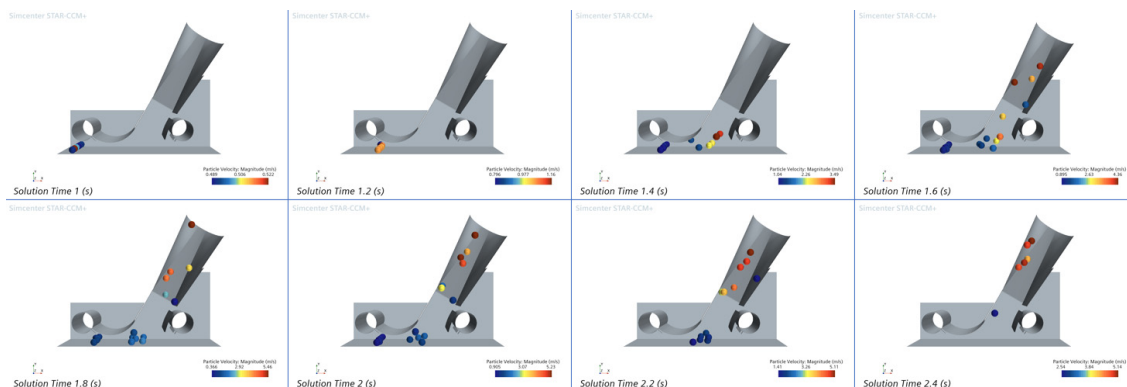


Fig.8. Particle collection process of circular tube nozzle collecting head

### 3.1. Influence of nozzle shape and diameter on acquisition efficiency

The shape of the nozzle has a direct influence on the effect of jet lifting particles, and the working efficiency of the collecting head is significantly different due to the different shape of the nozzle. The commonly used jet nozzle shapes mainly include round tubes and sheets, as shown in figure 9 and figure 10. The flow rate is set same, and the working parameters of different nozzle diameters and shapes are summarized in Table 2.

Table 2. Size and jet velocity of circular and flaky nozzles

Diameter of the circular tube nozzle (mm)	Jet velocity of circular tube nozzle (m/s)	Width of the blade nozzle (mm)	Jet velocity of blade nozzle (m/s)
12	17.8	5	8.68
14	13.1	8	5.42
16	10.0	11	3.95
18	7.9	14	3.10
20	6.4	17	2.55

Fig. 11 and Fig. 12 show the collection time and extreme stress of nodules with nozzle shape and diameter under different working conditions. With the increase of the nozzle diameter, the collection efficiency of the circular pipe nozzle gradually decreases, and the collection is completed in about 3s. The collection efficiency of the flaking nozzle is low, and the total collection time is about 12s, which decreases with the increase of the nozzle diameter. 12mm group and 14mm group have the best collection efficiency. The extreme stress graphs of the bottom decreased with the increase of the nozzle diameter, and the disturbance degree of the circular pipe nozzle to the bottom sediment was much higher than that of the sheet nozzle.

The numerical calculation shows that there is a significant wall attachment effect on the front and side nozzles of the collector head, forming a static region. The upwelling confluence position has a certain height relative to the bottom. The blade nozzle failed to lift the particles effectively. Since the flow velocity of the circular pipe

nozzle is larger, the lifting effect of the nodules is more significant, but the sediment disturbance is more obvious. Meanwhile, if the flow rate is kept constant, the flow rate will gradually decrease when the diameter increases, the lifting effect on the nodule will be weakened, and the disturbance to the sediment will also be reduced.

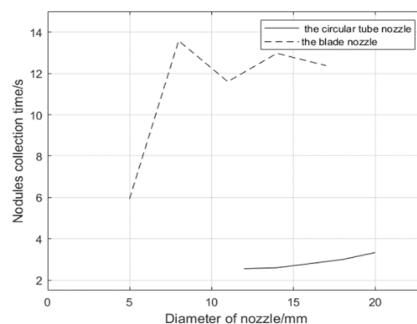


Fig.11. Nodules collection time of different structure

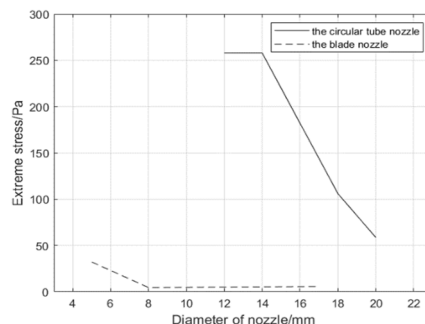


Fig.12. Extreme stress at seabed bottom

### 3.2. Influence of circular tube nozzle spacing on acquisition efficiency

When the collector is working, properly reducing the nozzle axis distance can improve the utilization rate of the nozzle and collection efficiency, but too dense nozzle distribution will increase the cost of construction and operation, reduce the energy conversion rate, and exacerbate the disturbance to the seabed environment. Table 3 shows the design conditions for different nozzle axis spacing.

**Table 3.** Working conditions of circular tube nozzle under different axis distance

Diameter of nozzle d (mm)	Nozzle axis distance h (mm)	Jet flow rate v (m/s)
12	24mm(1d)	9.14
12	30mm(1.5d)	11.64
12	36mm(2d)	14.09
12	42mm(2.5d)	16.05
12	50mm(3d)	19.89
14	35mm(1.5d)	9.92
14	42mm(2d)	11.82
14	49mm(2.5d)	13.78

Fig. 13 and Fig. 14 shows the the collection time and extreme stress of nodules with nozzle axis distance under two groups of nozzle diameters. Under 12mm diameter, the collection efficiency is best when the ratio h/d is 2. The collection efficiency increases first and then decreases with the increase of nozzle axis distance. The most efficient groups completed the collection in about 2.2 seconds. In contrast, the 14mm nozzle diameter group was not sensitive to the increase in nozzle spacing, and the collection was completed in about 2.5s.

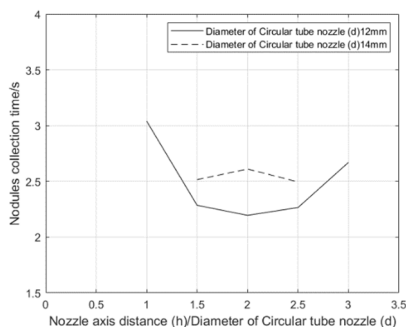


**Fig. 13.** Nodules collection time of different axis distance

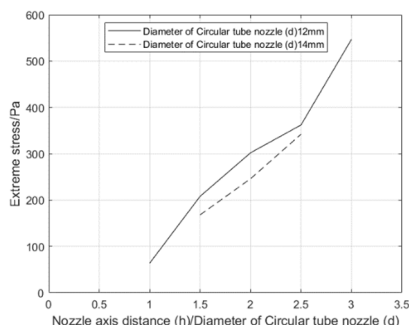


**Fig. 14.** Extreme stress at seabed bottom

In general, the nozzle axis distance has an important effect on the collection efficiency, and the optimal efficiency can be achieved by optimizing the nozzle axis distance and diameter. Both sets of data show that the extreme stress increases with the increase of nozzle axis distance. The extreme stress of the nozzle diameter 12mm is slightly higher than 14mm. When the nozzle spacing is large, there is a gap between the jets of the adjacent nozzle, which leads to the weakening of the lifting effect on the particles. If the nozzle spacing is too small, the adjacent nozzle jets interfere with each other, resulting in the

particle lifting is blocked, and the collection efficiency is reduced.

#### 4. Conclusion

In this paper, based on the double-jet hydraulic collector, the influence of three parameters of nozzle shape, nozzle size and nozzle axis distance was studied by numerical simulation method. The distribution characteristics of flow field and stress pressure were analyzed. Finally, the following conclusions were reached:

(1) Compared with the blade nozzle, the circular tube nozzle can play a more convergent role on the incoming jet, and the flow rate is relatively large, which has a more significant effect on the lifting of nodules. However, the stress pressure on the seabed bottom is also larger, which will cause more obvious disturbance to sediments. The circular tube nozzle is more helpful for collecting and lifting nodules. A circular tube nozzle with 12 or 14mm is selected in this study, which has relatively good collection performance.

(2) The influence of different nozzle axis distance on the collection capability and environmental disturbance of the device is analyzed, and the collection efficiency is optimal when the nozzle axis distance is 2 times the nozzle diameter.

#### Funding

This research was supported by funding “Guangdong Natural Capital Cooperation ([2024] No. 44)”

#### References

- J. Hein, K. Mizell, A. Koschinsky, T. Conrad, *Ore Geol. Rev.*, 51, 1-4 (2013)
- Z. Liu, K. Liu, X. Chen, Z. Ma, R. Lv, C. Wei, K. Ma, *Int J Min Sci Technol*, 33, 9, 1083-1115 (2023)
- S. Alhaddad, D. Mehta, R. Helmons, *RINENG*, 17, 100852 (2023)
- Z. Yue, G. Zhao, L. Xiao, M. Liu, *Appl Ocean Res.*, 110, 102606 (2021)
- L. Guan, D. Zhang, Y. Xia, J. Xia, *J. Ocean Technol.*, 40, 62-70 (2021)
- Q. Yang, S. Liu, X. Jiang, G. Liu, J. Xia, *The Ocean Engineering*. 41, 5, 181-192 (2023)
- D. Zhang, L. Guan, H. Cao, J. Xia, *J. Ocean Technol.*, 41, 4, 53-60 (2022)
- J. Liu, D. Xu, C. Ji, J. Xia, Q. Ran, *The Ocean Engineering*. 41, 3, 123-136 (2023)
- M. Wang, *The Development Of Deep Seafloor Solid Mineral Resources*, 310-312 (2015)
- X. Zhang, *Numerical Simulation of the Free Fall of Gravity Installed Anchor in Water*, 14-16 (2017)